

# DMSC: Dynamic Multi-Scale Coordination Framework for Time Series Forecasting

Haonan Yang<sup>1</sup>, Jianchao Tang<sup>1\*</sup>, Zhuo Li<sup>1</sup>, Long Lan<sup>1</sup>,

<sup>1</sup>College of Computer Science and Technology, National University of Defense Technology,

Changsha 410073, China

{yanghaonan21, tangjianchao14, lizhuo19, long.lan}@nudt.edu.cn

## Abstract

Time Series Forecasting (TSF) faces persistent challenges in modeling intricate temporal dependencies across different scales. Despite recent advances leveraging different decomposition operations and novel architectures based on CNN, MLP or Transformer, existing methods still struggle with static decomposition strategies, fragmented dependency modeling, and inflexible fusion mechanisms, limiting their ability to model intricate temporal dependencies. To explicitly solve the mentioned three problems respectively, we propose a novel Dynamic Multi-Scale Coordination Framework (DMSC) with Multi-Scale Patch Decomposition block (EMPD), Triad Interaction Block (TIB) and Adaptive Scale Routing MoE block (ASR-MoE). Specifically, EMPD is designed as a built-in component to dynamically segment sequences into hierarchical patches with exponentially scaled granularities, eliminating predefined scale constraints through input-adaptive patch adjustment. TIB then jointly models intra-patch, inter-patch, and cross-variable dependencies within each layer's decomposed representations. EMPD and TIB are jointly integrated into layers forming a multi-layer progressive cascade architecture, where coarse-grained representations from earlier layers adaptively guide fine-grained feature extraction in subsequent layers via gated pathways. And ASR-MoE dynamically fuses multi-scale predictions by leveraging specialized global and local experts with temporal-aware weighting. Comprehensive experiments on thirteen real-world benchmarks demonstrate that DMSC consistently maintains state-of-the-art (SOTA) performance and superior computational efficiency for TSF tasks.

## Introduction

Time Series Forecasting (TSF) constitutes a pivotal capability across numerous fields such as energy consumption (Alvarez et al. 2010; Guo et al. 2015), healthcare monitoring (Tran, Nguyen, and Shahabi 2019; Wei et al. 2022), transportation scheduling (Guo et al. 2020; Jin et al. 2021), weather forecasting (Bi et al. 2023; Wu et al. 2023b) and economics (Chen et al. 2023b; Yu et al. 2023). Time series data exhibit intricate temporal dependencies, which include nonlinear relationships, multi-scale patterns (e.g., trends and seasonality), and dynamic variable couplings (Qiu et al. 2024). Due to the inherent non-stationarity (Nason 2006) and complex interconnections (Dagum and Bianconcini

2016), traditional approaches often fail to adequately capture the underlying patterns in time series data, making effectively dependency modeling a critical challenge for enhancing predictive accuracy (Shao et al. 2025). In recent years, deep learning has demonstrated a strong capability to capture complex dependency relationships in time series data, making it a formidable tool for TSF (Chen et al. 2023a).

However, intricate dependencies in time series inherently manifest across multiscales: coarser granularities typically encapsulate long-term trends while finer resolutions capture short-term fluctuations and periodic patterns. Conventional single-scale modeling approaches often fail to balance fine-grained local details and holistic global trends (Wang et al. 2025). To effectively model multi-scale temporal dependencies, recent research has pioneered multi-scale modeling frameworks that concurrently extract global and local patterns, thereby thereby mitigating the representational constraints inherent in single-scale approaches. While previous implementations often employ moving average down-sampling (Wang et al. 2024b; Huang et al. 2025), which remains insufficient in capturing local semantic information. In contrast, more effective alternatives focus on patch-wise and variable-wise decomposition operations that decompose sequence across feature and temporal dimensions. Such decomposition operations better preserve both global trends and local semantics, and multi-length patches inherently facilitate the learning of multi-scale representations. Critically, prevailing methods suffer from two limitations: 1) reliance on fixed-scale decomposition strategies that lack dynamic scale adaptation; 2) fragmented processing of temporal dependencies and cross-variable interactions, which compromises holistic dependency modeling.

The primary advantage of multi-scale feature extraction lies in its capacity to mine complementary information across diverse temporal granularities and hierarchical levels, thereby overcoming the limitations of single-scale modeling. Following feature capture, the effective design of prediction heads for multi-scale fusion is equally important. Conventional approaches typically employ linear projection layers (Li, Li, and Diao 2025), additive combinations of multiple projections (Wang et al. 2024b), or spectral amplitude-weighted aggregation (Wu et al. 2023a). However, these simplistic fusion methods exhibit fundamental

\*Corresponding author

inadequacies: they fail to leverage heterogeneous dominance patterns across multiscales, disregard dynamic inter-scale importance, and incur quadratic growth of model parameters with increasing input lengths and scale counts, thereby severely compromising deployment efficiency (Qiu et al. 2024).

To effectively modeling complex temporal dependencies which inherently manifest across multiple patterns and scales, we propose a **Dynamic Multi-Scale Coordination framework (DMSC)** for TSF. This framework dynamically decomposes time series and extracts features across scales. It effectively captures intricate dependencies across temporal resolutions and cross-variable interactions. Meanwhile, it can generate adaptive predictions based on learned representations via temporal-aware fusion. Specifically, DMSC processes intricate dependencies through a multi-layer progressive architecture and an Adaptive Scale Routing Mixture-of-Experts (ASR-MoE). The multi-layer progressive cascade architecture incorporates Embedded Multi-Scale Patch Decomposition Block (EMPD), Triad Interaction Block (TIB), in which EMPD transforms the input into 3D representations at varying granularities and TIB models heterogeneous dependencies within each layer. In this architecture, coarse-grained representations from shallow layers adaptively guide fine-grained feature extraction in subsequent layers via gated pathways. After multi-scale feature extraction, ASR-MoE performs temporal-aware weighted dynamic fusion for multi-scale prediction, thus enabling adaptive integration of cross-scale features to enhancing forecasting accuracy. DMSC formulates a unified framework that incorporates dynamic patch decomposition, deeper models, and sparse MoE principles to achieve full-spectrum multi-scale coordination. This dynamic synergy enables the DMSC framework to achieve SOTA performance across 13 real-world benchmarks while maintaining high efficiency and low computational cost. Our contributions are as follows:

- A novel multi-layer progressive cascade architecture is designed to jointly integrate Embedded Multi-Scale Patch Decomposition Block (EMPD) and Triad Interaction Block (TIB) across layers. Unlike fixed-scale approaches, EMPD dynamically adjusts patch granularities by employing a lightweight network based on the temporal characteristics of input data, and TIB jointly models intra-patch, inter-patch, and inter-variable dependencies through gated feature fusion to form a coarse-to-fine feature pyramid, where coarse-grained representations from earlier layers adaptively guide fine-grained extraction in subsequent layers via gated residual pathways.
- Adaptive Scale Routing Mixture-of-Experts (ASR-MoE) is proposed to resolve static fusion limitations in prediction. It establishes a hierarchical expert architecture to explicitly decouples long-term and short-term dependencies, in which global-shared experts capture common long-term temporal dependencies, while local-specialized experts model different short-term variations. Significantly, a temporal-aware weighting aggregator is designed to dynamically compute scale-specific predic-

tion contributions with historical memory.

- Extensive experiments demonstrate that DMSC achieves SOTA performance and superior efficiency across multiple TSF benchmarks.

## Related Work

### Time Series Forecasting Models

Existing deep models for TSF tasks can be broadly categorized into MLP-based, CNN-based, and Transformer-based architectures (Wang et al. 2024c). MLP-based models (Chi et al. 2021; Oreshkin et al. 2020; Yi et al. 2023) typically capture temporal dependencies through predefined decomposition and fully-connected layers. While these models demonstrate efficiency in capturing intra-series patterns, they exhibit notable limitations in modeling long-term dependencies and complex inter-series relationships. In contrast, CNN-based models (Bai, Kolter, and Koltun 2018; LIU et al. 2022; Wang et al. 2023) leverage different convolutions to effectively capture local dependencies. Although they remain constrained in modeling global relationships, recent efforts have mitigated this through large-kernel convolutions (Luo and Wang 2024) and frequency-domain analysis (Wu et al. 2023a). Nevertheless, Transformer-based models (Wang et al. 2024a; Wu et al. 2021; Zhou et al. 2021) have emerged as a powerful paradigm, leveraging self-attention mechanisms (Vaswani et al. 2017) to effectively capture long-range dependencies and persistent temporal relationships. However, Transformer-based models face substantial criticism due to their permutation invariance and quadratic computational complexity limitations in recent researches (Tang and Zhang 2024; Zeng et al. 2023). Despite significant progress, most existing deep architectures rely on single or fixed decomposition strategies, and often model dependencies in a fragmented manner, lacking mechanisms for dynamic, adaptive multi-scale decomposition and coordinated dependency modeling.

### Decomposition Operations in TSF

To effectively capture intricate temporal dependencies, numerous studies have adopted a multi-scale modeling perspective, employing diverse decomposition operations on time series. TimesNet (Wu et al. 2023a) learns frequency-adaptive periods in the frequency domain and transforms series into 2D tensors, explicitly modeling intra-period and inter-period variations. TimeMixer (Wang et al. 2024b) decomposes sequences into seasonal and trend components (Wu et al. 2021), then applies mixing strategies at different granularities to integrate multi-scale features. However, simply using moving average inadequately preserves local semantic patterns. Diverging from these operations, several methods focus on variable-wise and patch-wise disentanglement. PatchTST (Nie et al. 2023) segments series into subseries-level patches as input tokens and employs channel independence to capture local semantics. ITransformer (Liu et al. 2024) embeds entire series as single tokens to model extended global representations. TimeXer (Wang et al. 2024d) hierarchically represents variables through dual

disentanglement, variable-wise for cross-channel interactions and patch-wise for endogenous variables. However, these decomposition techniques are constrained by static or predefined scale settings, hindering their adaptability to complex temporal patterns.

### Multi-Scale Prediction Operations in TSF

Beyond multi-scale decomposition operations, researchers have also investigated multi-scale operations in prediction heads. TimeMixer (Wang et al. 2024b) employs dedicated projectors to generate scale-specific predictions. Diverging from simplistic additive aggregation, TimeMixer++ (Wang et al. 2025) utilizes frequency-domain amplitude analysis to perform weighted aggregation of projector outputs. TimeKAN (Huang et al. 2025) adopts frequency transformation and padding operations to unify multi-scale representations into identical dimensions, thereby enabling holistic scale integration. Current multi-scale fusion mechanisms predominantly rely on static weighting or fixed designs. They fail to dynamically prioritize the importance of different scales with intricate temporal dependencies. Different from these fragmented approaches, our proposed DMSC framework explores full-spectrum multi-scale coordination across embedding, extraction, and prediction stages, achieving both superior forecasting accuracy and high computational efficiency.

## Dynamic Multi-Scale Coordination Framework

Time series forecasting addresses the fundamental challenge of predicting future values  $Y = y_{t+1}, \dots, y_{t+h} \in \mathbb{R}^{h \times C}$  from historical observations  $X = x_1, \dots, x_t \in \mathbb{R}^{t \times C}$ , where  $h$  is the prediction horizon,  $t$  is the history horizon, and  $C$  is the number of variables. To model complex multi-scale dependencies inherent in real-world time series, we propose the Dynamic Multi-Scale Coordination (DMSC) framework. As illustrated in Fig. 1, DMSC establishes full-spectrum multi-scale coordination across three key stages: embedding, feature extraction, and prediction, realized through EMPD, TIB and ASR-MoE components.

### Multi-Layer Progressive Cascade Architecture

The multi-layer progressive cascade architecture facilitates hierarchical feature learning through stacked EMPD-TIB units, forming a dynamic feature pyramid. Within this pyramid, coarse-grained representations from earlier layers adaptively guide fine-grained feature extraction in subsequent layers via gated pathways. Formally, given input  $\mathbf{X} \in \mathbb{R}^{C \times L}$ , the  $l$ -th layer processes:

$$\begin{aligned} \mathcal{T} &= \{\mathbf{F}_1, \mathbf{F}_2, \dots, \mathbf{F}_l\}, \\ \mathbf{F}_l &= \mathbf{TIB}_l(\mathbf{Z}_l), \\ \mathbf{Z}_l &= \mathbf{EMPD}_l(\mathcal{G}_l(\mathbf{F}_{l-1}) + \mathbf{X}), \end{aligned} \quad (1)$$

where  $\mathcal{T}$  denotes the set of hierarchical features generated by this architecture for ASR-MoE, with each  $\mathbf{F}_l \in \mathbb{R}^{C \times D}$  representing the output of  $l$ -th layer. Here,  $\mathcal{G}_l$  represents a

gated projection matrix that adaptively modulates the residual information flow. This cascade flow enables progressive refinement of multi-scale representations, where  $\mathbf{F}_{l-1}$  adaptively guides the computation of  $\mathbf{Z}_l$  with residual connections, and  $\mathbf{TIB}_l$  iteratively enhances representations by jointly modeling intra-patch, inter-patch, and cross-variable dependencies. By combining dynamic patch decomposition (EMPD) with triadic dependency modeling (TIB), our cascade architecture achieves input-aware progressive refinement of temporal granularities. This integration enables coherent modeling of both short-term dynamics and long-range trends while maintaining parameter efficiency.

### Embedded Multi-Scale Patch Decomposition

Patch decomposition serves as a fundamental operation that transforms time series into structured representations, preserving local semantics while enabling hierarchical pattern discovery. Unlike conventional single or fixed-scale approaches, the EMPD block introduces adaptive and hierarchical decomposition mechanism as a built-in component, dynamically adjusting patch granularities based on sequence characteristics. This approach eliminates rigid predefined patch configurations while natively integrating multi-scale decomposition into our framework.

Specifically, given an input time series tensor  $\mathbf{X} \in \mathbb{R}^{C \times L}$  (where  $C$  denotes the number of variates and  $L$  the sequence length), EMPD first computes a scale factor  $\alpha$  through a lightweight neural network:

$$\alpha = \mathcal{N}_\theta(\Phi_{\text{GAP}}(\mathbf{X})) \quad (2)$$

where  $\mathcal{N}_\theta$  denotes a lightweight MLP with sigmoid activation, and  $\Phi_{\text{GAP}}$  denotes a global average pooling operation that compresses the temporal dimension. The factor  $\alpha \in [0, 1]$  dynamically determines the base patch length, which subsequently undergoes exponential decay across layers as follows:

$$\begin{aligned} \mathbf{P}_{\text{base}} &= [\mathbf{P}_{\min} + \alpha \cdot (\mathbf{P}_{\max} - \mathbf{P}_{\min})], \\ \mathbf{P}_l &= \max(\mathbf{P}_{\min}, [\mathbf{P}_{\text{base}} / \tau^l]), \end{aligned} \quad (3)$$

where  $\mathbf{P}_{\max}$  and  $\mathbf{P}_{\min}$  denote the parameters for minimum and maximum patch bounds, respectively.  $\mathbf{P}_l$  represents the patch length at the  $l$ -th layer. This design ensures that shallow layers process coarse-grained dependencies while deeper layers capture fine-grained ones. EMPD then applies replication padding to mitigate boundary effects, followed by hierarchical patch unfolding operation:

$$\mathbf{X}_p^l = \text{Unfold}_{P_l, S_l}(\text{Padding}_{S_l}(X)), \quad (4)$$

where  $\text{Padding}_{S_l}(\cdot)$  denotes the replication padding operation with stride  $S_l = P_l/2$  and  $\text{Unfold}_{P_l, S_l}$  unfolds the padded sequence into patches of length  $P_l$  using a stride of  $S_l$ . This operation produces a 3D patch tensor  $\mathbf{X}_p^l \in \mathbb{R}^{C \times N_l \times P_l}$ . Finally, EMPD projects  $\mathbf{X}_p^l$  into a unified embedding space via a linear projection:

$$\mathbf{Z}^l = \text{Projector}(\mathbf{X}_p^l), \quad (5)$$

This direct linear projection efficiently maps patch-wise temporal features into a unified embedding space, avoiding redundant flattening operations while preserving the hierarchical structure of the multi-scale patches.

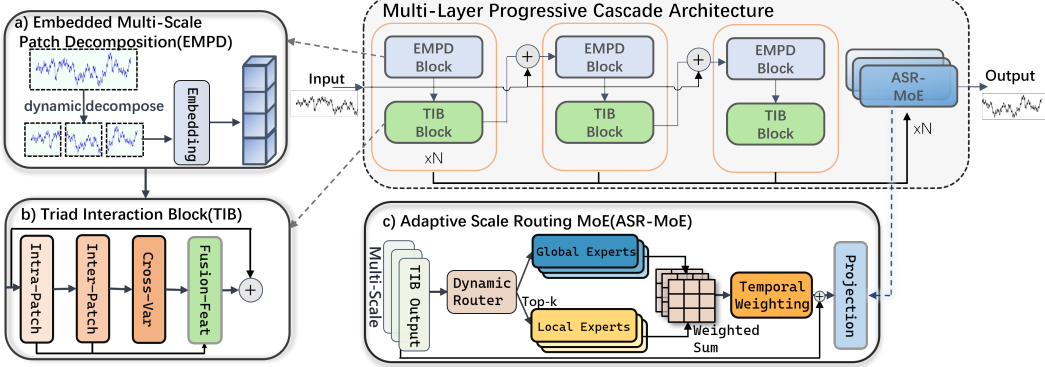


Figure 1: The framework of DMSC. EMPD dynamically segments input series into hierarchical patches, TIB jointly models three dependencies, and ASR-MoE fuses multi-scale predictions adaptively.

### Triad Interaction Block

The Triad Interaction Block (TIB) is designed to model heterogeneous dependencies within the multi-scale patch representations generated by EMPD, through joint capture of intra-patch, inter-patch, and cross-variable interactions. Given the input tensor  $\mathbf{Z}^l \in \mathbb{R}^{C \times N_l \times D}$ , TIB integrates these three complementary dependency types within a coherent framework. Specifically, TIB first processes intra-patch dependencies using depth-wise separable convolutions through operation  $\zeta_{\text{intra}}$  to capture fine-grained local patterns:

$$\mathbf{F}_{\text{intra}}^l = \zeta_{\text{intra}}(\mathbf{Z}^l), \quad (6)$$

where  $\zeta_{\text{intra}}$  comprises depth-wise convolution and Conv1d to capture local temporal contexts and project features back to the embedding space. This operation preserves intra-patch continuity while effectively extracting local representations.

For inter-patch dynamics  $\mathbf{F}_{\text{inter}}^l$ , TIB employs dilated convolutions with adaptive pooling via  $\zeta_{\text{inter}}$ :

$$\mathbf{F}_{\text{inter}}^l = \zeta_{\text{inter}}(\mathbf{F}_{\text{intra}}^l), \quad (7)$$

where  $\zeta_{\text{inter}}$  consists of the dilated convolution and adaptive pooling operations, capturing broader temporal contexts and patch-level information without increasing computational cost.

TIB then models cross-variable dependencies by generating adaptive weighting coefficients  $\mathbf{G}^l \in \mathbb{R}^{C \times 1}$  as follows:

$$\begin{aligned} \mathbf{G}^l &= \sigma(\text{MLP}(\bar{\mathbf{F}}_{\text{inter}}^l)), \\ \mathbf{F}_{\text{cross}}^l &= \mathbf{G}^l \odot \mathbf{F}_{\text{inter}}^l, \end{aligned} \quad (8)$$

where  $\bar{\mathbf{F}}_{\text{inter}}^l$  denotes the global average of  $\mathbf{F}_{\text{inter}}^l$ , and the sigmoid function  $\sigma$  acts as a feature-specific gate mechanism.  $\mathbf{G}^l$  are applied element-wise to  $\mathbf{F}_{\text{inter}}^l$  via the Hadamard product  $\odot$ , adaptively scaling each feature's contribution based on its global relevance and enabling context-aware cross-variable interactions.

Finally, the three dependency representations are adaptively fused using learned gating weights, and the resulting features are integrated with residual connection and normalization:

$$\mathbf{F}_{\text{fused}}^l = \sum_{i=1}^3 \mathbf{G}_i^l \odot \mathbf{F}_i^l,$$

$$\mathbf{F}_{\text{output}}^l = \text{LayerNorm}(\mathbf{F}_{\text{fused}}^l + \mathbf{Z}^l), \quad (9)$$

where  $\mathbf{G}_i^l$  represents the learned gating weights for the  $i$ -th representations. This architecture enables TIB to dynamically balance the contributions of different dependency types based on the temporal characteristics of input data. Consequently, it effectively captures intricate dependencies and provides rich temporal features for multi-scale prediction.

### Adaptive Scale Routing Mixture-of-Experts

To address the limitations of static fusion mechanisms in multi-scale forecasting, we propose the Adaptive Scale Routing Mixture-of-Experts (ASR-MoE) block. This dynamic prediction head captures temporal dependencies at different horizons through a hierarchy of experts (global-shared and local-specialized experts) and adaptively aggregates scale-specific predictions based on temporal patterns.

Specifically, ASR-MoE incorporates two distinct expert groups to handle different temporal granularities. Global experts  $\mathcal{E}^g = \{\mathcal{G}_1, \mathcal{G}_2, \dots, \mathcal{G}_m\}$  capture common long-term dependencies through deeper networks, modeling persistent trends and long-periodic patterns that commonly existed in time series. Local experts  $\mathcal{E}^l = \{\mathcal{L}_1, \mathcal{L}_2, \dots, \mathcal{L}_n\}$  capture diverse short-term variations via shallower networks, detecting short-periodic patterns and high-frequency fluctuations that vary dynamically across stages. This explicit decoupling enables specialized handling of complex temporal dynamics while maintaining high parameter efficiency.

To compute the weighting for experts at each scale, a dynamic routing mechanism assigns input-dependent weights, thereby balancing the contributions of global and local dependencies. Given a scale-specific feature  $\mathbf{F}_l$ , the router generates weights, and only the top- $K$  local experts are activated via sparse routing:

$$\hat{\Omega}_l^L, \mathcal{I} = \begin{cases} \Omega_l^L, & \Omega_l^L \in \text{Top-K}(\Omega_l, K) \\ 0, & \text{otherwise} \end{cases}$$

$$\begin{aligned} \Omega_G &= \text{Sigmoid}(\text{MLP}(\mathbf{F}_l)), \\ \Omega_l &= \text{Softmax}(\text{MLP}(\mathbf{F}_l)), \end{aligned} \quad (10)$$

where  $\Omega_g$  and  $\Omega_l$  represent the global and local expert weight matrices, respectively.  $\mathcal{I}$  denotes the set of indices

Models	DMSC(Ours)	TimeMixer	iTransformer	PatchTST	Dlinear	TimesNet	Autoformer	TimeXer	PatchMLP	TimeKAN	AMD
Metric	MSE	MAE	MSE	MAE	MSE	MAE	MSE	MAE	MSE	MAE	MSE
ETTh1	<b>0.415</b> <b>0.426</b>	0.456 0.444	0.452 0.446	0.445 0.445	0.461 0.457	0.479 0.466	0.670 0.564	0.460 0.452	0.458 0.445	0.429 0.432	0.452 0.439
ETTh2	<b>0.355</b> <b>0.383</b>	<u>0.372</u> <u>0.400</u>	0.384 0.407	0.383 0.412	0.563 0.519	0.411 0.421	0.488 0.494	0.374 0.404	0.406 0.422	0.389 0.409	0.616 0.558
ETTm1	<b>0.368</b> <b>0.383</b>	0.384 0.398	0.408 0.412	0.386 0.400	0.404 0.408	0.418 0.418	0.636 0.534	0.391 0.395	0.387 0.398	<u>0.376</u> <u>0.397</u>	0.394 <u>0.396</u>
ETTm2	<b>0.268</b> <b>0.317</b>	0.278 0.324	0.292 0.336	0.288 0.334	0.354 0.402	0.291 0.330	0.502 0.452	<u>0.277</u> <u>0.323</u>	0.287 0.329	0.282 0.330	0.288 0.332
Electricity	<b>0.170</b> <b>0.258</b>	0.190 0.280	<u>0.176</u> <u>0.265</u>	0.205 0.295	0.226 0.319	0.194 0.293	0.492 0.523	0.201 0.275	0.200 0.296	0.201 0.290	0.206 0.287
Exchange	<b>0.336</b> <b>0.391</b>	0.359 <u>0.401</u>	0.362 0.406	0.389 0.417	<u>0.339</u> 0.414	0.430 0.446	0.539 0.519	0.398 0.422	0.383 0.417	0.384 0.414	0.366 0.408
Weather	<b>0.233</b> <b>0.269</b>	0.245 0.274	0.261 0.281	0.258 0.279	0.265 0.316	0.256 0.283	0.348 0.382	<u>0.242</u> <u>0.272</u>	0.252 0.277	0.244 0.274	0.271 0.291
Traffic	<b>0.407</b> <b>0.274</b>	0.509 0.307	<u>0.422</u> <u>0.283</u>	0.482 0.309	0.688 0.428	0.633 0.334	1.028 0.605	0.466 0.287	0.539 0.364	0.590 0.373	0.547 0.345
Solar	<b>0.213</b> <b>0.258</b>	0.228 0.279	0.238 <u>0.263</u>	0.249 0.292	0.330 0.401	0.268 0.286	0.727 0.634	<u>0.226</u> 0.269	0.298 0.301	0.289 0.321	0.363 0.337

Table 1: Long-term forecasting results. All the results are averaged from 4 different prediction lengths {96, 192, 336, 720}, and the look-back length is fixed to 96 for all baselines. A lower MSE or MAE indicates a better prediction, with the best in boldface and second in underline.

Models	DMSC(Ours)	TimeMixer	iTransformer	PatchTST	Dlinear	TimesNet	Autoformer	TimeXer	PatchMLP	TimeKAN	AMD
Metric	MSE	MAE	MSE	MAE	MSE	MAE	MSE	MAE	MSE	MAE	MSE
PEMS03	<b>0.131</b> <b>0.241</b>	0.190 0.288	0.261 0.328	0.308 0.368	0.279 0.377	<u>0.154</u> <u>0.254</u>	0.513 0.517	0.180 0.280	0.220 0.289	0.283 0.357	0.281 0.368
PEMS04	<b>0.129</b> <b>0.244</b>	0.230 0.324	0.913 0.801	0.365 0.405	0.295 0.389	<u>0.138</u> <u>0.250</u>	0.472 0.495	0.327 0.418	0.203 0.305	0.297 0.372	0.327 0.397
PEMS07	<u>0.092</u> <u>0.193</u>	0.165 0.256	0.109 0.214	0.438 0.422	0.329 0.394	0.109 0.216	0.418 0.466	<b>0.088</b> <b>0.192</b>	0.166 0.262	0.264 0.346	0.196 0.318
PEMS08	<b>0.162</b> <b>0.228</b>	0.264 0.332	0.199 0.278	0.347 0.390	0.403 0.444	<u>0.198</u> <u>0.236</u>	0.603 0.541	0.206 0.248	0.244 0.326	0.337 0.377	0.427 0.443

Table 2: Short-term forecasting results. All the results are averaged from 4 different prediction lengths {12, 24, 48, 96}, and the look-back length is fixed to 96 for all baselines.

for the selected experts. Finally, a temporal-aware weighting module fuses outputs from all scales by historical scale importance. The scale-specific predictions  $\hat{\mathbf{Y}}^l$  are fused using time-dependent weights:

$$\mathbf{w} = \text{Softmax} \left( \text{MLP} \left( \bigoplus_{l=1}^L \phi(\mathbf{F}_l) \cdot \mathbf{w}_{\text{hist}} \right) \right), \quad (11)$$

where  $\phi(\cdot)$  denotes temporal descriptors,  $\mathbf{w}_{\text{hist}}$  represents the historical weighting memory, and  $\bigoplus$  denotes the concatenation operation. The final prediction is obtained by integrating the multi-scale outputs:

$$\hat{\mathbf{Y}} = \sum_{l=1}^L \mathbf{w}_l \left( \sum_{m=1}^{m=1} \Omega_m^G \mathcal{G}_m(\mathbf{F}_l) + \sum_{n \in \mathcal{I}} \hat{\Omega}_n^L \mathcal{L}_n(\mathbf{F}_l) \right), \quad (12)$$

To ensure balanced expert utilization, ASR-MoE incorporates an auxiliary balance loss:

$$\mathcal{L}_{\text{balance}} = -\lambda \mathbf{E}[\sum \Omega_j \log \Omega_j], \quad (13)$$

The overall loss function for DMSC is defined as follows:

$$\mathcal{L} = \mathcal{L}_{\text{pred}} + \mathcal{L}_{\text{balance}}, \quad (14)$$

where  $\mathcal{L}_{\text{pred}}$  denotes the Mean Squared Error (MSE) loss.

By integrating hierarchical expert specialization, dynamic routing, and temporal-aware weighting, ASR-MoE adaptively prioritizes relevant scales and experts, achieving a synergistic balance between long-term trend capture and short-term detail refinement in time series forecasting.

## Experiments

To comprehensively evaluate the performance and effectiveness of the proposed DMSC framework, we conduct extensive experiments on 13 real-world TSF benchmarks across multiple domains and temporal resolutions.

**Datasets.** For long-term forecasting, we conduct experiments on nine well-established benchmarks, including ETT (ETTh1, ETTh2, ETTm1, ETTm2), Electricity, ECL, Traffic, Weather and Solar. For short-term forecasting, we utilize the PEMS (PEMS03, PEMS04, PEMS07, PEMS08) dataset.

**Baselines.** We compare our framework with ten SOTA models of TSF, including transformer-based models: iTransformer (Liu et al. 2024), PatchTST (Nie et al. 2023), Autoformer (Wu et al. 2021), TimeXer (Wang et al. 2024d); MLP-based models: DLinear (Zeng et al. 2023), PatchMLP (Tang and Zhang 2024), AMD (Hu et al. 2025); CNN-based models: TimesNet (Wu et al. 2023a), TimeMixer (Wang et al. 2024b), and a novel architecture TimeKAN (Huang et al. 2025).

## Main Results

The main results for long-term and short-term forecasting are presented in Table 1 and Table 2, in which the lower MSE and MAE values indicate superior forecasting performance. The proposed DMSC framework demonstrates consistent SOTA performance across all 13 benchmarks, achieving the lowest MAE and MSE in most experimental settings. These results confirm the robust effectiveness and general-

izability of DMSC for both long-term and short-term forecasting tasks. Notably, multi-scale architectures like TimesNet and PatchMLP exhibit performance instability, which we attribute to their inflexible fusion mechanisms that fails to fully leverage the captured multi-scale features. The competitive performance of TimeXer and iTransformer underscores the effectiveness of patch-wise and variate-wise strategy for information representation, but their fixed decomposition schemes inherently constrain the model’s potential. Furthermore, compared to iTransformer and Dlinear, DMSC achieves considerable improvement in data with more variate(Traffic, PEMS), highlighting the necessity of jointly dependency modeling. Collectively, the above observations validate the efficacy of DMSC in addressing the core challenges of time series forecasting.

## Model Analysis

**Ablation Study.** To rigorously evaluate the contribution and effectiveness of each component within DMSC, we conduct systematic ablation experiments on Electricity, Weather, Traffic and Solar datasets. We first ablate each of the three core blocks individually. Results of Table 3 highlight the complementary synergy of the three blocks. We then perform further ablation analyses for individual components. For EMPD in Table 4, ① employs predefined static patch size for exponentially decaying. For TIB in Table 5, ② retains only intra-patch feature extraction without jointly modeling the three dependency representations, while ③ removes dynamic fusion mechanism  $\mathbf{F}_{\text{fused}}^l$  in TIB. For ASR-MoE in Table 6, ④ replace the prediction heads with a simple summation of multiple linear layers, and ⑤ and ⑥ eliminate global experts and local experts respectively. Based on these ablation studies, we have the following observations.

Dateset	Electricity		Weather		Traffic		Solar	
Metric	MSE	MAE	MSE	MAE	MSE	MAE	MSE	MAE
DMSC(Ours)	<b>0.170</b>	<b>0.258</b>	<b>0.233</b>	<b>0.269</b>	<b>0.407</b>	<b>0.274</b>	<b>0.213</b>	<b>0.258</b>
w/o EMPD	0.181	0.270	0.248	0.275	0.503	0.323	0.248	0.278
w/o TIB	0.185	0.273	0.255	0.278	0.497	0.321	0.264	0.293
w/o ASR-MoE	0.196	0.285	0.251	0.280	0.503	0.320	0.271	0.305

Table 3: Ablation results. All results are averaged from prediction length {96, 192, 336, 720}.

For EMPD, replacing the input-adaptive decomposition with either predefined static patches or raw data embedding leads to performance degradation. This demonstrates the necessity of adaptive patch-wise decomposition and its lightweight network for dynamic granularity adjustment. For TIB, replacing joint modeling with standard convolution layers or only intra-patch features resulted in performance drops, validating the necessity of comprehensive joint modeling of triadic dependencies. Similarly, ablation of dynamic fusion mechanism in TIB confirms its effectiveness in fusing heterogeneous dependencies, as static handling undermines holistic cross-scale dependency capture. For ASR-MoE, replacing the adaptive prediction mechanism with a single prediction head or summed multiple linear projections leads to

Case	Electricity		Weather		Traffic		Solar	
	MSE	MAE	MSE	MAE	MSE	MAE	MSE	MAE
DMSC(Ours)	<b>0.170</b>	<b>0.258</b>	<b>0.233</b>	<b>0.269</b>	<b>0.407</b>	<b>0.274</b>	<b>0.213</b>	<b>0.258</b>
①static decomp	0.179	0.271	0.245	0.272	0.478	0.313	0.243	0.276

Table 4: Ablation study on EMPD to compare dynamic decomposition with static predefined decomposition strategies.

Case	Electricity		Weather		Traffic		Solar	
	MSE	MAE	MSE	MAE	MSE	MAE	MSE	MAE
DMSC(Ours)	<b>0.170</b>	<b>0.258</b>	<b>0.233</b>	<b>0.269</b>	<b>0.407</b>	<b>0.274</b>	<b>0.213</b>	<b>0.258</b>
②only $\mathbf{F}_{\text{intra}}$	0.187	0.276	0.249	0.275	0.489	0.315	0.275	0.298
③w/o $\mathbf{F}_{\text{fused}}^l$	0.186	0.277	0.247	0.273	0.483	0.314	0.277	0.299

Table 5: Ablation study on TIB to validate effectiveness of joint triad dependency modeling.

Case	Electricity		Weather		Traffic		Solar	
	MSE	MAE	MSE	MAE	MSE	MAE	MSE	MAE
DMSC(Ours)	<b>0.170</b>	<b>0.258</b>	<b>0.233</b>	<b>0.269</b>	<b>0.407</b>	<b>0.274</b>	<b>0.213</b>	<b>0.258</b>
④Agg. Heads	0.194	0.281	0.254	0.281	0.510	0.312	0.278	0.299
⑤w/o $\mathcal{E}^g$	0.191	0.280	0.250	0.279	0.504	0.324	0.265	0.293
⑥w/o $\mathcal{E}^l$	0.199	0.285	0.243	0.271	0.488	0.326	0.275	0.303

Table 6: Ablation study on ASR-MoE to assess the importance of expert specialization (global/local) and dynamic fusion strategies for prediction results.

substantial performance declines. This indicates that single heads inadequately utilize multi-scale features, while simplistic aggregation overlooks scale-specific dependency importance. Moreover, removing either global or local experts degrades performance, demonstrating the necessity of maintaining distinct experts for different temporal patterns. The elaborate design of ASR-MoE effectively harnesses diverse temporal dynamics through collective specialized expert utilization. Collectively, these ablation studies confirm that dynamic and multi-scale modeling is central to DMSC. All of three blocks and the proposed progressive cascade architecture together enable robust multiscale modeling and hierarchical feature learning, with consistent performance drops from ablating any component validate architectural integrity of DMSC.

**ASR-MoE Expert Specialization.** To verify the specialization of ASR-MoE experts, we visualize their activation patterns across different temporal experts. As shown in Fig. 2, distinct specialization profiles emerge: global experts exhibit heightened sensitivity to persistent trends and long-periodic patterns, whereas local experts demonstrate acute responsiveness to short-periodic patterns and high-frequency fluctuations. This observed specialization demonstrates the adaptive acquisition of specialized knowledge by different experts.

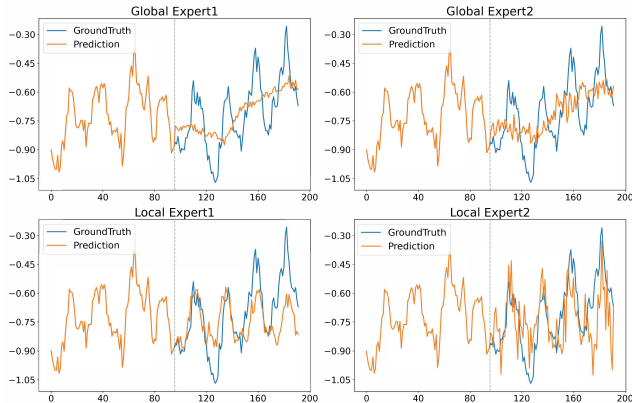


Figure 2: Visualization of different experts on ETTh1 datasets, the look-back and prediction length are set to 96.

**Increasing Look-Back Length.** Theoretically, longer input sequences provide richer historical information, which can enhance the model’s ability to capture long-term trends and complex multi-scale dependencies. Our DMSC framework is specifically designed to leverage this characteristic, as its dynamic multi-scale coordination capability inherently facilitates adaptive modeling and effective information utilization across varying look-back lengths. So we evaluate DMSC with look-back lengths selected from  $\{48, 96, 192, 336, 720\}$  on Electricity dataset. As shown in Fig. 3, DMSC consistently achieves improved performance with longer historical sequences while outperforming other baseline methods. This demonstrates its capacity to extract richer temporal representations from extended contexts and effectively integrate multi-scale temporal patterns.

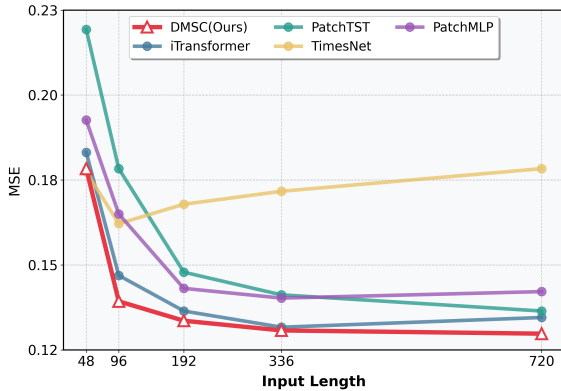


Figure 3: Forecasting results with varying look-back length on Electricity dataset. Look-back lengths are set to  $\{48, 96, 192, 336, 720\}$ , and prediction length is fixed to 96.

**Efficiency Analysis** We rigorously evaluate the memory usage and training time of DMSC against other SOTA baselines on Weather(21 variates) and Traffic(862 variates) datasets. As demonstrated in Fig. 4 and Fig. 5, DMSC consistently achieves superior efficiency in both memory usage

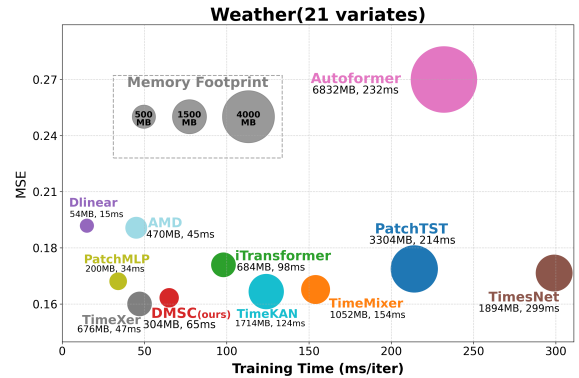


Figure 4: Model efficiency analysis under 96-look-back length and 96-prediction length on Weather(21 variates) datasets. Batch size is set to 128.

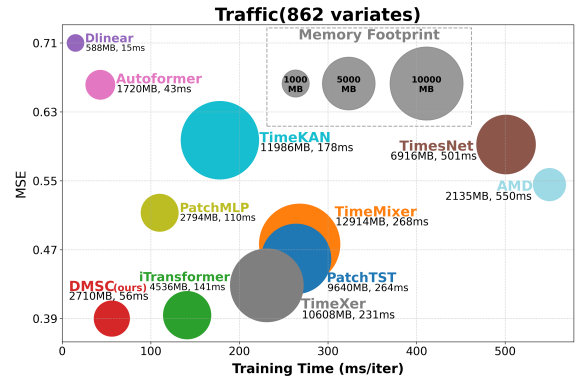


Figure 5: Model efficiency analysis under 96-look-back length and 96-prediction length on Traffic(862 variates) datasets. Batch size is set to 16.

and training time while maintaining competitive forecasting accuracy. Crucially, DMSC demonstrates near-linear scalability to long sequences, as outperforming Transformer-based models with quadratic complexity and MLP-based approaches susceptible to parameter explosion. These efficiency gains are particularly pronounced when processing high-dimensional multivariate data (Traffic), where the cross-variable interaction in TIB avoids the computational overhead of exhaustive pairwise attention while preserving modeling capacity. DMSC thus establishes a balance of accuracy, latency, and memory usage for practical deployment scenarios.

## Conclusion

This paper presents the Dynamic Multi-Scale Coordination (DMSC) framework, a novel approach that advances time series forecasting through comprehensive dynamic multi-scale coordination. DMSC has three key contributions: 1) Embedded Multi-Scale Patch Decomposition(EMPD) dynamically decomposes time series into hierarchical patches, eliminating predefined scale constraints through input-adaptive granularity adjustment; 2) Triad Interaction Block

(TIB) jointly models intra-patch, inter-patch, and cross-variable dependencies, forming a coarse-to-fine feature pyramid through progressive cascade layers; 3) Adaptive Scale Routing MoE (ASR-MoE) dynamically fuses multi-scale predictions via temporal-aware weighting of specialized global and local experts. Extensive experiments on thirteen benchmarks demonstrate that DMSC achieves SOTA performance and superior efficiency. Future work will extend the framework to multi-task learning and explore optimizations on complex real-world environments, thereby enhancing its applicability across diverse scenarios.

## References

Alvarez, F. M.; Troncoso, A.; Riquelme, J. C.; and Ruiz, J. S. A. 2010. Energy time series forecasting based on pattern sequence similarity. *IEEE Transactions on Knowledge and Data Engineering*, 23(8): 1230–1243.

Bai, S.; Kolter, J. Z.; and Koltun, V. 2018. An Empirical Evaluation of Generic Convolutional and Recurrent Networks for Sequence Modeling. arXiv:1803.01271.

Bi, K.; Xie, L.; Zhang, H.; Chen, X.; Gu, X.; and Tian, Q. 2023. Accurate medium-range global weather forecasting with 3D neural networks. *Nature*, 619(7970): 533–538.

Chen, Z.; Ma, M.; Li, T.; Wang, H.; and Li, C. 2023a. Long sequence time-series forecasting with deep learning: A survey. *Information Fusion*, 97: 101819.

Chen, Z.; Zheng, L.; Lu, C.; Yuan, J.; and Zhu, D. 2023b. ChatGPT Informed Graph Neural Network for Stock Movement Prediction. *SSRN Electronic Journal*.

Chi, H.; Liu, F.; Yang, W.; Lan, L.; Liu, T.; Han, B.; Cheung, W.; and Kwok, J. 2021. TOHAN: A one-step approach towards few-shot hypothesis adaptation. *Advances in neural information processing systems*, 34: 20970–20982.

Dagum, E. B.; and Bianconcini, S. 2016. *Seasonal Adjustment Methods and Real Time Trend-Cycle Estimation*, volume 8. Springer Nature.

Guo, C.; Yang, B.; Andersen, O.; Jensen, C. S.; and Torp, K. 2015. Ecomark 2.0: empowering eco-routing with vehicular environmental models and actual vehicle fuel consumption data. *GeoInformatica*, 19(3): 567–599.

Guo, C.; Yang, B.; Hu, J.; Jensen, C. S.; and Chen, L. 2020. Context-aware, preference-based vehicle routing. *The VLDB Journal*, 29(5): 1149–1170.

Hu, Y.; Liu, P.; Zhu, P.; Cheng, D.; and Dai, T. 2025. Adaptive Multi-Scale Decomposition Framework for Time Series Forecasting. arXiv:2406.03751.

Huang, S.; Zhao, Z.; Li, C.; and Bai, L. 2025. TimeKAN: KAN-based Frequency Decomposition Learning Architecture for Long-term Time Series Forecasting. arXiv:2502.06910.

Jin, K.; Wi, J.; Lee, E.; Kang, S.; Kim, S.; and Kim, Y. 2021. TrafficBERT: Pre-trained model with large-scale data for long-range traffic flow forecasting. *Expert Systems with Applications*, 186: 115738.

Li, C.; Li, M.; and Diao, R. 2025. TVNet: A Novel Time Series Analysis Method Based on Dynamic Convolution and 3D-Variation. arXiv:2503.07674.

LIU, M.; Zeng, A.; Chen, M.; Xu, Z.; LAI, Q.; Ma, L.; and Xu, Q. 2022. SCINet: Time Series Modeling and Forecasting with Sample Convolution and Interaction. In *Advances in Neural Information Processing Systems*, volume 35, 5816–5828.

Liu, Y.; Hu, T.; Zhang, H.; Wu, H.; Wang, S.; Ma, L.; and Long, M. 2024. iTransformer: Inverted Transformers Are Effective for Time Series Forecasting. arXiv:2310.06625.

Luo, D.; and Wang, X. 2024. Moderntcn: A modern pure convolution structure for general time series analysis. In *The twelfth international conference on learning representations*, 1–43.

Nason, G. P. 2006. Stationary and non-stationary time series. In *Statistics in Volcanology*. Geological Society of London.

Nie, Y.; Nguyen, N. H.; Sinhong, P.; and Kalagnanam, J. 2023. A Time Series is Worth 64 Words: Long-term Forecasting with Transformers. In *11th International Conference on Learning Representations, ICLR 2023*.

Oreshkin, B. N.; Carpov, D.; Chapados, N.; and Bengio, Y. 2020. N-BEATS: Neural basis expansion analysis for interpretable time series forecasting. arXiv:1905.10437.

Qiu, X.; Hu, J.; Zhou, L.; Wu, X.; Du, J.; Zhang, B.; Guo, C.; Zhou, A.; Jensen, C. S.; Sheng, Z.; and Yang, B. 2024. TFB: Towards Comprehensive and Fair Benchmarking of Time Series Forecasting Methods. *Proceedings of the VLDB Endowment*, 2363–2377.

Shao, Z.; Wang, F.; Xu, Y.; Wei, W.; Yu, C.; Zhang, Z.; Yao, D.; Sun, T.; Jin, G.; Cao, X.; Cong, G.; Jensen, C. S.; and Cheng, X. 2025. Exploring Progress in Multivariate Time Series Forecasting: Comprehensive Benchmarking and Heterogeneity Analysis. *IEEE Transactions on Knowledge and Data Engineering*, 291–305.

Tang, P.; and Zhang, W. 2024. Unlocking the Power of Patch: Patch-Based MLP for Long-Term Time Series Forecasting. arXiv:2405.13575.

Tran, L.; Nguyen, M.; and Shahabi, C. 2019. Representation learning for early sepsis prediction. In *2019 Computing in Cardiology (CinC)*, 1–4. IEEE.

Vaswani, A.; Shazeer, N.; Parmar, N.; Uszkoreit, J.; Jones, L.; Gomez, A. N.; Kaiser, Ł.; and Polosukhin, I. 2017. Attention is all you need. *Advances in neural information processing systems*, 30.

Wang, H.; Peng, J.; Huang, F.; Wang, J.; Chen, J.; and Xiao, Y. 2023. MICN: Multi-scale Local and Global Context Modeling for Long-term Series Forecasting. In *11th International Conference on Learning Representations, ICLR 2023*.

Wang, J.; Xia, X.; Lan, L.; Wu, X.; Yu, J.; Yang, W.; Han, B.; and Liu, T. 2024a. Tackling noisy labels with network parameter additive decomposition. *IEEE Transactions on Pattern Analysis and Machine Intelligence*, 46(9): 6341–6354.

Wang, S.; Li, J.; Shi, X.; Ye, Z.; Mo, B.; Lin, W.; Ju, S.; Chu, Z.; and Jin, M. 2025. TimeMixer++: A General Time Series Pattern Machine for Universal Predictive Analysis. arXiv:2410.16032.

Wang, S.; Wu, H.; Shi, X.; Hu, T.; Luo, H.; Ma, L.; Zhang, J. Y.; and Zhou, J. 2024b. TimeMixer: Decomposable Multiscale Mixing for Time Series Forecasting. arXiv:2405.14616.

Wang, Y.; Wu, H.; Dong, J.; Liu, Y.; Long, M.; and Wang, J. 2024c. Deep Time Series Models: A Comprehensive Survey and Benchmark. arXiv:2407.13278.

Wang, Y.; Wu, H.; Dong, J.; Qin, G.; Zhang, H.; Liu, Y.; Qiu, Y.; Wang, J.; and Long, M. 2024d. TimeXer: Empowering Transformers for Time Series Forecasting with Exogenous Variables. arXiv:2402.19072.

Wei, K.; Li, T.; Huang, F.; Chen, J.; and He, Z. 2022. Cancer classification with data augmentation based on generative adversarial networks. *Frontiers of Computer Science*, 16(2): 162601.

Wu, H.; Hu, T.; Liu, Y.; Zhou, H.; Wang, J.; and Long, M. 2023a. TimesNet: Temporal 2D-Variation Modeling for General Time Series Analysis. In *11th International Conference on Learning Representations, ICLR 2023*.

Wu, H.; Xu, J.; Wang, J.; and Long, M. 2021. Autoformer: Decomposition transformers with auto-correlation for long-term series forecasting. *Advances in neural information processing systems*, 34: 22419–22430.

Wu, H.; Zhou, H.; Long, M.; and Wang, J. 2023b. Interpretable weather forecasting for worldwide stations with a unified deep model. *Nature Machine Intelligence*, 5(6): 602–611.

Yi, K.; Zhang, Q.; Fan, W.; Wang, S.; Wang, P.; He, H.; An, N.; Lian, D.; Cao, L.; and Niu, Z. 2023. Frequency-domain MLPs are more effective learners in time series forecasting. *Advances in Neural Information Processing Systems*, 36: 76656–76679.

Yu, X.; Chen, Z.; Ling, Y.; Dong, S.; Liu, Z.; and Lu, Y. 2023. Temporal data meets LLM-explainable financial time series forecasting.

Zeng, A.; Chen, M.; Zhang, L.; and Xu, Q. 2023. Are transformers effective for time series forecasting? In *Proceedings of the AAAI conference on artificial intelligence*, volume 37, 11121–11128.

Zhou, H.; Zhang, S.; Peng, J.; Zhang, S.; Li, J.; Xiong, H.; and Zhang, W. 2021. Informer: Beyond efficient transformer for long sequence time-series forecasting. In *Proceedings of the AAAI conference on artificial intelligence*, volume 35, 11106–11115.

## Implementation Details

### Dataset Descriptions

We conduct long-term forecasting experiments on 9 real-world datasets, including ETT(ETTh1, ETTh2, ETTm1, ETTm2); Electricity(ECL); Exchange; Solar; Traffic; and Weather datasets. Meanwhile, we use PEMS(PEMS03, PEM04, PEM07, PEM08) datasets to conduct short-term forecasting experiments. The details of datasets are listed in Tab 7.

### Metrics Details

To evaluate model’s performance for TSF, we utilize the mean square error(MSE) and mean absolute error(MAE). The calculations of metrics are as follows:

$$\text{MSE} = \frac{1}{n} \sum_{i=1}^n (\mathbf{Y}_i - \hat{\mathbf{Y}}_i)^2 \quad (15)$$

$$\text{MAE} = \frac{1}{n} \sum_{i=1}^n |\mathbf{Y}_i - \hat{\mathbf{Y}}_i| \quad (16)$$

### Implementation Details

All experiments are implemented in Pytorch, and conducted on a single NVIDIA RTX 4090 24GB GPU. We utilize ADAM optimizer with an initial learning rate  $10^{-3}$  and L2 loss for model optimization. For DMSC, we set layers of progressive cascade framework to 2 - 5, embedding dimension is set to 64, 128, 256, 512. The patch decay rate is set to 2 for exponentially degradation. All experiments are based on the framework of TimesNet. And all the baselines are implemented based on the configurations of original paper and its code.

## Model Analysis

### Model Complexity Analysis

The computational complexity of DMSC is dominated by three core components: EMPD, TIB, and ASR-MoE. EMPD hierarchically decomposes input sequences into exponentially scaled patches via unfolding and linear projection, yielding a lightweight  $O(C \cdot L \cdot d_{\text{model}})$  complexity, where  $C$  is the number of variate,  $L$  is the sequence length, and  $d_{\text{model}}$  is the embedding dimension. TIB employs depth-wise separable convolutions and dilated convolutions to model intra-patch, inter-patch, and cross-variable dependencies, maintaining near-linear complexity  $O(C \cdot N \cdot d_{\text{model}}^2)$  per layer ( $N$  is patch count). ASR-MoE leverages sparse activation, routing each input to only top- $K$  experts (global and local), reducing fusion complexity from quadratic to  $O(B \cdot C \cdot d_{\text{model}} \cdot (K + S))$  ( $B$ : batch size,  $S$ : shared experts). Collectively, DMSC achieves  $O(L)$  sequential scalability, outperforming Transformer-based models( $O(L^2)$ ) and MLP-based alternatives( $O(L \cdot d_{ff}^2)$ ), while excelling in both long- and short-term forecasting tasks.

### Hyperparameter Sensitivity Analysis

**Embedding Dimension.** The embedding dimension determines the richness of feature representations. We evaluate the model’s performance on ECL and Weather datasets with embedding dimensions  $d_{\text{model}} \in \{64, 128, 256, 512\}$ . The results in Fig. 6a and Fig. 6b show that the optimal dimension is at 128 / 256, as smaller embedding impairs multi-scale feature separation, while larger configurations yield marginal gains with higher memory cost, indicating dimensionality saturating.

Name	Domain	Length	Num	Prediction Length	Dataset Size	Freq. (m)
ETTh1	Temperature	14400	7	{96,192,336,720}	(8545,2881,2881)	60
ETTh2	Temperature	14400	7	{96,192,336,720}	(8545,2881,2881)	60
ETTm1	Temperature	57600	7	{96,192,336,720}	(34465,11521,11521)	15
ETTm2	Temperature	57600	7	{96,192,336,720}	(34465,11521,11521)	15
Electricity	Electricity	26304	321	{96,192,336,720}	(18317,2633,5261)	60
Exchange	Exchange Rate	7588	8	{96,192,336,720}	(5120,665,1422)	1440
Traffic	Road Occupancy	17544	862	{96,192,336,720}	(12185,1757,3509)	60
Weather	Weather	52696	21	{96,192,336,720}	(36792,5271,10540)	10
Solar-Energy	Energy	52179	137	{96,192,336,720}	(36601,5161,10417)	10
PEMS03	Traffic Flow	26208	358	{12,24,48,96}	(15617,5135,5135)	5
PEMS04	Traffic Flow	16992	307	{12,24,48,96}	(10172,3375,3375)	5
PEMS07	Traffic Flow	28224	883	{12,24,48,96}	(16711,5622,5622)	5
PEMS08	Traffic Flow	17856	170	{12,24,48,96}	(10690,3548,3548)	5

Table 7: Dataset Descriptions. Num is the number of variable. Dataset size is organized in (Train, Validation, Test).

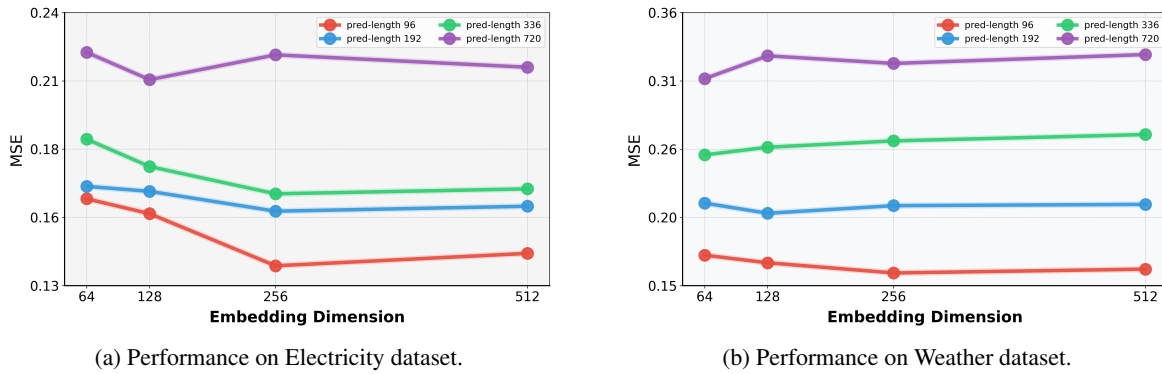


Figure 6: Hyperparameter sensitivity analysis under different embedding dimension,  $d_{\text{model}}$  is set to  $\{64, 128, 256, 512\}$ . Left is conducted on Electricity dataset and right is on Weather dataset. Look-back length is fixed to 96, and prediction lengths are set to  $\{96, 192, 336, 720\}$ .

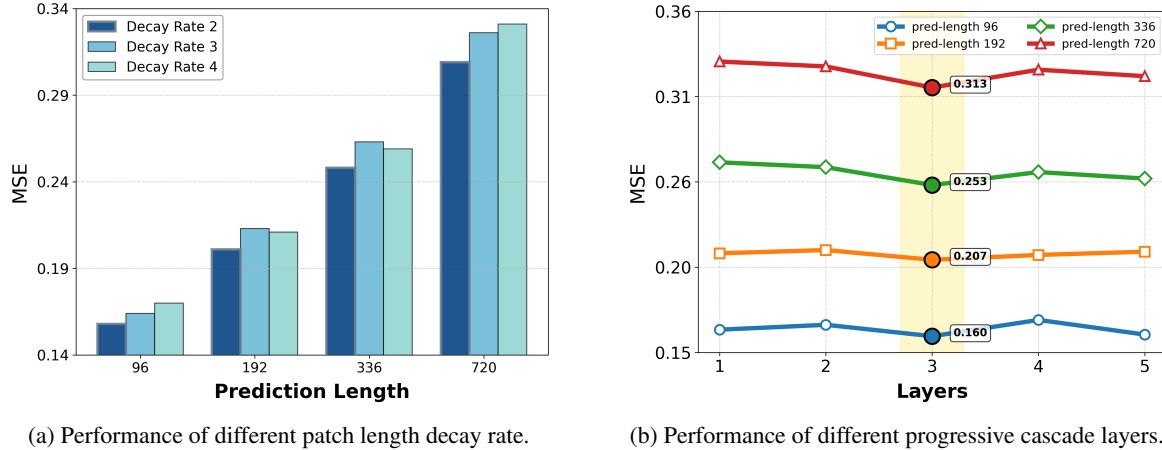


Figure 7: Hyperparameter sensitivity analysis on Weather dataset. Left shows performance of different patch length decay rate, right shows performance of different progressive cascade layers. Look-back length is fixed to 96, and prediction lengths are set to  $\{96, 192, 336, 720\}$ .

**EMPD Patch Length Decay.** EMPD employs exponentially decaying patch lengths across layers to capture multi-

scale dependencies. We evaluate the impact of the EMPD decay rate by testing values of  $\tau \in \{2, 3, 4\}$  on Weather

dataset. As shown in Fig. 7a, a decay factor of  $\tau = 2$  achieves the best forecasting performance, which balances the preservation of sufficient local details in fine-grained layers with the extraction of broader trends in coarse-grained layers.

**Number of Progressive Cascade Layers.** The number of progressive cascade layers ( $l \in \{1, 2, 3, 4, 5\}$ ) influences hierarchical feature extraction. As shown in Fig. 7b, three layers can achieve optimal efficiency, shallower stacks (1 - 2 layers) fail to capture fine-grained interactions, while deeper configurations (4 - 5 layers) introduce substantially increased latency with diminishing performance returns.

## Full Results

We evaluate DMSC on 13 real-world TSF benchmarks spanning diverse domains. Tab 8 shows the full results of long-term forecasting tasks on ETT (ETTh1, ETTh2, ETTm1, ETTm2), Electricity, ECL, Traffic, Weather and Solar datasets. Tab 9 contains the full results of short-term forecasting tasks on PEMS (PEMS03, PEMS04, PEMS07, PEMS08) datasets. From full results, we can see that DMSC achieves pretty good performance on most datasets and tasks.

Meanwhile, Tab 10 shows the full results of ablation study on Electricity, Weather, Traffic and Solar datasets, which demonstrating the efficiency and contribution of each component in DMSC.

Models	DMSC(Ours)	TimeMixer	iTransformer	PatchTST	Dlinear	TimesNet	Autoformer	TimeXer	PatchMLP	TimeKAN	AMD	
Metric	MSE	MAE	MSE	MAE	MSE	MAE	MSE	MAE	MSE	MAE	MSE	MAE
ETTh1	96	<b>0.370</b> <u>0.395</u>	0.379 <u>0.397</u>	0.387 <u>0.405</u>	0.378 <u>0.399</u>	0.397 <u>0.412</u>	0.415 <u>0.429</u>	0.589 <u>0.526</u>	0.386 <u>0.404</u>	0.393 <u>0.405</u>	0.387 <u>0.401</u>	0.394 <u>0.404</u>
	192	<b>0.408</b> <u>0.420</u>	0.430 <u>0.429</u>	0.441 <u>0.436</u>	0.427 <u>0.429</u>	0.446 <u>0.441</u>	0.479 <u>0.466</u>	0.653 <u>0.551</u>	0.429 <u>0.435</u>	0.443 <u>0.434</u>	0.415 <u>0.423</u>	0.444 <u>0.432</u>
	336	<b>0.421</b> <u>0.433</u>	0.493 <u>0.459</u>	0.494 <u>0.463</u>	0.468 <u>0.455</u>	0.489 <u>0.467</u>	0.517 <u>0.482</u>	0.715 <u>0.581</u>	0.484 <u>0.457</u>	0.486 <u>0.456</u>	0.453 <u>0.443</u>	0.485 <u>0.451</u>
	720	<b>0.462</b> <u>0.457</u>	0.522 <u>0.493</u>	0.488 <u>0.483</u>	0.508 <u>0.497</u>	0.513 <u>0.511</u>	0.505 <u>0.490</u>	0.726 <u>0.601</u>	0.544 <u>0.513</u>	0.509 <u>0.487</u>	<b>0.461</b> <u>0.463</u>	0.486 <u>0.472</u>
	Avg	<b>0.415</b> <u>0.426</u>	0.456 <u>0.444</u>	0.452 <u>0.446</u>	0.445 <u>0.445</u>	0.461 <u>0.457</u>	0.479 <u>0.466</u>	0.670 <u>0.564</u>	0.460 <u>0.452</u>	0.458 <u>0.445</u>	0.429 <u>0.432</u>	0.452 <u>0.439</u>
ETTh2	96	<b>0.275</b> <u>0.329</u>	0.290 <u>0.341</u>	0.301 <u>0.350</u>	0.295 <u>0.347</u>	0.341 <u>0.394</u>	0.316 <u>0.358</u>	0.443 <u>0.459</u>	0.284 <u>0.337</u>	0.311 <u>0.358</u>	0.291 <u>0.342</u>	0.397 <u>0.451</u>
	192	<b>0.359</b> <u>0.383</u>	0.366 <u>0.394</u>	0.380 <u>0.399</u>	0.378 <u>0.401</u>	0.482 <u>0.479</u>	0.415 <u>0.414</u>	0.500 <u>0.506</u>	0.366 <u>0.391</u>	0.404 <u>0.415</u>	0.376 <u>0.393</u>	0.501 <u>0.501</u>
	336	<b>0.376</b> <u>0.398</u>	0.425 <u>0.433</u>	0.423 <u>0.431</u>	0.425 <u>0.442</u>	0.591 <u>0.541</u>	0.452 <u>0.448</u>	0.506 <u>0.502</u>	0.438 <u>0.438</u>	0.447 <u>0.451</u>	0.437 <u>0.443</u>	0.611 <u>0.563</u>
	720	0.412 <u>0.424</u>	<b>0.405</b> <u>0.431</u>	0.431 <u>0.447</u>	0.436 <u>0.456</u>	0.839 <u>0.661</u>	0.461 <u>0.463</u>	0.503 <u>0.509</u>	0.407 <u>0.449</u>	0.462 <u>0.464</u>	0.451 <u>0.458</u>	0.956 <u>0.718</u>
	Avg	<b>0.355</b> <u>0.383</u>	0.372 <u>0.400</u>	0.384 <u>0.407</u>	0.383 <u>0.412</u>	0.563 <u>0.519</u>	0.411 <u>0.421</u>	0.488 <u>0.494</u>	0.374 <u>0.404</u>	0.406 <u>0.422</u>	0.389 <u>0.409</u>	0.616 <u>0.558</u>
ETTm1	96	<b>0.304</b> <u>0.335</u>	0.319 <u>0.359</u>	0.341 <u>0.376</u>	0.326 <u>0.366</u>	0.346 <u>0.374</u>	0.336 <u>0.375</u>	0.564 <u>0.506</u>	0.318 <u>0.356</u>	0.321 <u>0.362</u>	0.326 <u>0.365</u>	0.331 <u>0.363</u>
	192	<b>0.346</b> <u>0.364</u>	0.360 <u>0.384</u>	0.382 <u>0.396</u>	0.365 <u>0.387</u>	0.382 <u>0.391</u>	0.377 <u>0.395</u>	0.586 <u>0.516</u>	0.373 <u>0.389</u>	0.364 <u>0.381</u>	0.360 <u>0.384</u>	0.373 <u>0.382</u>
	336	0.372 <u>0.392</u>	0.395 <u>0.406</u>	0.420 <u>0.421</u>	0.392 <u>0.406</u>	0.415 <u>0.415</u>	0.418 <u>0.420</u>	0.679 <u>0.547</u>	0.412 <u>0.387</u>	0.396 <u>0.404</u>	<b>0.369</b> <u>0.402</u>	0.405 <u>0.403</u>
	720	0.451 <u>0.440</u>	0.461 <u>0.444</u>	0.487 <u>0.456</u>	0.461 <u>0.443</u>	0.473 <u>0.451</u>	0.541 <u>0.481</u>	0.715 <u>0.567</u>	0.460 <u>0.450</u>	0.468 <u>0.443</u>	<b>0.449</b> <u>0.437</u>	0.467 <u>0.437</u>
	Avg	<b>0.368</b> <u>0.383</u>	0.384 <u>0.398</u>	0.408 <u>0.412</u>	0.386 <u>0.400</u>	0.404 <u>0.408</u>	0.418 <u>0.418</u>	0.636 <u>0.534</u>	0.391 <u>0.395</u>	0.387 <u>0.398</u>	0.376 <u>0.397</u>	0.394 <u>0.396</u>
ETTm2	96	<u>0.174</u> <b>0.256</b>	0.179 <u>0.261</u>	0.186 <u>0.272</u>	0.184 <u>0.269</u>	0.193 <u>0.293</u>	0.188 <u>0.268</u>	0.554 <u>0.469</u>	<b>0.172</b> <u>0.254</u>	0.176 <u>0.259</u>	0.176 <u>0.263</u>	0.187 <u>0.271</u>
	192	<b>0.233</b> <u>0.295</u>	0.238 <u>0.301</u>	0.252 <u>0.312</u>	0.247 <u>0.307</u>	0.284 <u>0.361</u>	0.250 <u>0.306</u>	0.609 <u>0.497</u>	0.241 <u>0.302</u>	0.246 <u>0.304</u>	0.239 <u>0.301</u>	0.251 <u>0.309</u>
	336	<b>0.296</b> <u>0.331</u>	0.299 <u>0.339</u>	0.315 <u>0.351</u>	0.313 <u>0.354</u>	0.382 <u>0.429</u>	0.306 <u>0.341</u>	0.401 <u>0.409</u>	0.301 <u>0.340</u>	0.309 <u>0.344</u>	0.304 <u>0.346</u>	0.309 <u>0.346</u>
	720	<b>0.370</b> <u>0.385</u>	0.395 <u>0.394</u>	0.415 <u>0.408</u>	0.409 <u>0.406</u>	0.558 <u>0.525</u>	0.420 <u>0.405</u>	0.443 <u>0.433</u>	0.394 <u>0.395</u>	0.417 <u>0.408</u>	0.410 <u>0.408</u>	0.407 <u>0.400</u>
	Avg	<b>0.268</b> <u>0.317</u>	0.278 <u>0.324</u>	0.292 <u>0.336</u>	0.288 <u>0.334</u>	0.354 <u>0.402</u>	0.291 <u>0.330</u>	0.502 <u>0.452</u>	<b>0.277</b> <u>0.323</u>	0.287 <u>0.329</u>	0.282 <u>0.330</u>	0.288 <u>0.332</u>
Electricity	96	<b>0.138</b> <u>0.223</u>	0.161 <u>0.252</u>	<b>0.148</b> <u>0.241</u>	0.181 <u>0.274</u>	0.211 <u>0.302</u>	0.163 <u>0.267</u>	0.232 <u>0.347</u>	0.241 <u>0.244</u>	0.167 <u>0.264</u>	0.177 <u>0.270</u>	0.185 <u>0.267</u>
	192	<u>0.160</u> <b>0.258</b>	0.176 <u>0.269</u>	0.167 <u>0.248</u>	0.187 <u>0.280</u>	0.211 <u>0.305</u>	0.184 <u>0.284</u>	0.363 <u>0.447</u>	<b>0.159</b> <u>0.260</u>	0.181 <u>0.276</u>	0.185 <u>0.276</u>	0.190 <u>0.272</u>
	336	<b>0.167</b> <u>0.253</u>	0.193 <u>0.283</u>	<u>0.179</u> <b>0.271</b>	0.204 <u>0.296</u>	0.223 <u>0.319</u>	0.196 <u>0.297</u>	0.599 <u>0.595</u>	0.177 <u>0.276</u>	0.203 <u>0.303</u>	0.201 <u>0.292</u>	0.205 <u>0.288</u>
	720	0.213 <u>0.299</u>	0.232 <u>0.316</u>	<b>0.208</b> <u>0.298</u>	0.246 <u>0.328</u>	0.258 <u>0.351</u>	0.232 <u>0.325</u>	0.775 <u>0.701</u>	0.229 <u>0.321</u>	0.251 <u>0.341</u>	0.241 <u>0.323</u>	0.246 <u>0.321</u>
	Avg	<b>0.170</b> <u>0.258</u>	0.190 <u>0.280</u>	0.176 <u>0.265</u>	0.205 <u>0.295</u>	0.226 <u>0.319</u>	0.194 <u>0.293</u>	0.492 <u>0.523</u>	0.201 <u>0.275</u>	0.200 <u>0.296</u>	0.201 <u>0.290</u>	0.206 <u>0.287</u>
Exchange	96	<b>0.082</b> <u>0.201</u>	0.087 <u>0.204</u>	0.088 <u>0.208</u>	0.094 <u>0.213</u>	0.098 <u>0.233</u>	0.115 <u>0.242</u>	0.158 <u>0.290</u>	0.094 <u>0.214</u>	0.094 <u>0.217</u>	0.092 <u>0.212</u>	0.088 <u>0.208</u>
	192	<b>0.174</b> <u>0.298</u>	<u>0.177</u> <b>0.295</b>	0.180 <u>0.303</u>	0.182 <u>0.303</u>	0.186 <u>0.325</u>	0.216 <u>0.333</u>	0.299 <u>0.406</u>	0.182 <u>0.303</u>	0.187 <u>0.311</u>	0.180 <u>0.300</u>	0.182 <u>0.305</u>
	336	<b>0.315</b> <u>0.405</u>	0.328 <u>0.414</u>	0.331 <u>0.418</u>	0.347 <u>0.426</u>	<u>0.325</u> <u>0.434</u>	0.375 <u>0.444</u>	0.470 <u>0.511</u>	0.384 <u>0.448</u>	0.342 <u>0.424</u>	0.352 <u>0.430</u>	0.332 <u>0.417</u>
	720	0.772 <u>0.659</u>	0.847 <u>0.692</u>	0.848 <u>0.695</u>	0.931 <u>0.724</u>	<b>0.746</b> <u>0.663</u>	1.012 <u>0.765</u>	1.228 <u>0.869</u>	0.932 <u>0.724</u>	0.908 <u>0.715</u>	0.912 <u>0.715</u>	0.861 <u>0.701</u>
	Avg	<b>0.336</b> <u>0.391</u>	0.359 <u>0.401</u>	0.362 <u>0.406</u>	0.389 <u>0.417</u>	0.339 <u>0.414</u>	0.430 <u>0.446</u>	0.539 <u>0.519</u>	0.398 <u>0.422</u>	0.383 <u>0.417</u>	0.384 <u>0.414</u>	0.366 <u>0.408</u>
Weather	96	<u>0.160</u> <b>0.210</b>	0.164 <u>0.210</u>	0.176 <u>0.216</u>	0.174 <u>0.215</u>	0.195 <u>0.252</u>	0.172 <u>0.221</u>	0.301 <u>0.364</u>	<b>0.157</b> <u>0.205</u>	0.168 <u>0.214</u>	0.163 <u>0.210</u>	0.194 <u>0.236</u>
	192	<b>0.207</b> <u>0.250</u>	0.208 <u>0.251</u>	0.225 <u>0.257</u>	0.221 <u>0.256</u>	0.239 <u>0.299</u>	0.220 <u>0.260</u>	0.335 <u>0.385</u>	<b>0.204</b> <u>0.248</u>	0.215 <u>0.255</u>	0.209 <u>0.251</u>	0.239 <u>0.271</u>
	336	<b>0.253</b> <u>0.284</u>	0.264 <u>0.292</u>	0.281 <u>0.299</u>	0.280 <u>0.297</u>	0.282 <u>0.333</u>	0.280 <u>0.302</u>	0.352 <u>0.376</u>	0.264 <u>0.293</u>	0.272 <u>0.295</u>	0.263 <u>0.291</u>	0.290 <u>0.306</u>
	720	<b>0.313</b> <u>0.332</u>	0.343 <u>0.343</u>	0.361 <u>0.353</u>	0.357 <u>0.349</u>	0.345 <u>0.381</u>	0.353 <u>0.350</u>	0.405 <u>0.401</u>	0.343 <u>0.343</u>	0.351 <u>0.346</u>	<b>0.341</b> <u>0.344</u>	0.362 <u>0.352</u>
	Avg	<b>0.233</b> <u>0.269</u>	0.245 <u>0.274</u>	0.261 <u>0.281</u>	0.258 <u>0.279</u>	0.265 <u>0.316</u>	0.256 <u>0.283</u>	0.348 <u>0.382</u>	0.242 <u>0.272</u>	0.252 <u>0.277</u>	0.244 <u>0.274</u>	0.271 <u>0.291</u>
Traffic	96	<b>0.389</b> <u>0.259</u>	0.476 <u>0.292</u>	<u>0.393</u> <b>0.269</b>	0.459 <u>0.299</u>	0.712 <u>0.438</u>	0.593 <u>0.317</u>	0.663 <u>0.403</u>	0.428 <u>0.271</u>	0.513 <u>0.352</u>	0.598 <u>0.382</u>	0.546 <u>0.346</u>
	192	<b>0.405</b> <u>0.258</u>	0.501 <u>0.301</u>	<u>0.412</u> <b>0.277</b>	0.469 <u>0.303</u>	0.662 <u>0.417</u>	0.618 <u>0.327</u>	0.915 <u>0.557</u>	0.447 <u>0.280</u>	0.509 <u>0.350</u>	0.579 <u>0.365</u>	0.529 <u>0.335</u>
	336	<b>0.398</b> <u>0.286</u>	0.514 <u>0.314</u>	<u>0.424</u> <b>0.283</b>	0.483 <u>0.309</u>	0.669 <u>0.419</u>	0.642 <u>0.341</u>	1.217 <u>0.704</u>	0.472 <u>0.289</u>	0.533 <u>0.360</u>	0.572 <u>0.361</u>	0.540 <u>0.339</u>
	720	<b>0.437</b> <u>0.290</u>	0.545 <u>0.320</u>	<u>0.459</u> <u>0.301</u>	0.518 <u>0.326</u>	0.709 <u>0.437</u>	0.679 <u>0.350</u>	1.317 <u>0.755</u>	0.517 <u>0.307</u>	0.599 <u>0.395</u>	0.609 <u>0.384</u>	0.576 <u>0.358</u>
	Avg	<b>0.407</b> <u>0.274</u>	0.509 <u>0.307</u>	<u>0.422</u> <b>0.283</b>	0.482 <u>0.309</u>	0.688 <u>0.428</u>	0.633 <u>0.334</u>	1.028 <u>0.605</u>	0.466 <u>0.287</u>	0.539 <u>0.364</u>	0.590 <u>0.373</u>	0.547 <u>0.345</u>
Solar	96	<u>0.187</u> <b>0.231</b>	0.196 <u>0.263</u>	0.207 <u>0.237</u>	0.216 <u>0.274</u>	0.290 <u>0.378</u>	0.223 <u>0.256</u>	0.552 <u>0.524</u>	0.198 <u>0.244</u>	0.239 <u>0.272</u>	0.248 <u>0.302</u>	0.310 <u>0.312</u>
	192	<b>0.216</b> <u>0.261</u>	0.245 <u>0.279</u>	0.242 <u>0.264</u>	0.250 <u>0.294</u>	0.320 <u>0.398</u>	0.262 <u>0.272</u>	0.696 <u>0.605</u>	0.226 <u>0.270</u>	0.291 <u>0.298</u>	0.291 <u>0.321</u>	0.348 <u>0.330</u>
	336	<b>0.223</b> <u>0.269</u>	0.235 <u>0.287</u>	<u>0.251</u> <b>0.274</b>	0.265 <u>0.302</u>	0.353 <u>0.415</u>	0.287 <u>0.299</u>	0.816 <u>0.677</u>	0.239 <u>0.281</u>	0.325 <u>0.316</u>	0.307 <u>0.332</u>	0.399 <u>0.355</u>
	720	<b>0.226</b> <u>0.271</u>	0.236 <u>0.286</u>	0.251 <u>0.276</u>	0.266 <u>0.298</u>	0.357 <u>0.413</u>						

Models	DMSC(Ours)	TimeMixer	iTransformer	PatchTST	Dlinear	TimesNet	Autoformer	TimeXer	PatchMLP	TimeKAN	AMD	
Metric	MSE	MAE	MSE	MAE	MSE	MAE	MSE	MAE	MSE	MAE	MSE	MAE
PEMS03	12	<b>0.066</b> <b>0.171</b>	0.084 0.194	0.069 <u>0.175</u>	0.105 0.216	0.122 0.245	0.088 0.195	0.224 0.346	0.068 0.179	0.118 0.191	0.095 0.210	0.106 0.225
	24	<u>0.092</u> <b>0.203</b>	0.130 0.244	0.099 0.210	0.198 0.296	0.202 0.320	0.118 0.224	0.492 0.513	<b>0.089</b> <u>0.204</u>	0.204 0.231	0.166 0.281	0.174 0.294
	48	<b>0.136</b> <b>0.251</b>	0.218 0.317	0.164 0.275	0.472 0.466	0.334 0.428	0.169 0.268	0.392 0.459	0.137 <u>0.253</u>	0.213 0.314	0.314 0.393	0.333 0.417
	96	<b>0.230</b> <u>0.339</u>	0.327 0.398	0.711 0.651	0.458 0.493	0.459 0.517	<u>0.239</u> <b>0.330</b>	0.944 0.749	0.427 0.483	0.347 0.421	0.558 0.543	0.510 0.536
Avg		<b>0.131</b> <b>0.241</b>	0.190 0.288	0.261 0.328	0.308 0.368	0.279 0.377	0.154 0.254	0.513 0.517	0.180 0.280	0.220 0.289	0.283 0.357	0.281 0.368
PEMS04	12	<b>0.078</b> <b>0.183</b>	0.105 0.216	0.766 0.709	0.116 0.230	0.147 0.272	<u>0.092</u> <u>0.202</u>	0.211 0.341	0.293 0.397	0.109 0.204	0.107 0.222	0.131 0.256
	24	<b>0.102</b> <b>0.215</b>	0.168 0.280	0.799 0.728	0.216 0.314	0.225 0.340	<u>0.111</u> <u>0.224</u>	0.394 0.471	0.308 0.409	0.129 0.248	0.178 0.294	0.196 0.311
	48	<b>0.147</b> <b>0.261</b>	0.270 0.359	1.041 0.882	0.503 0.489	0.356 0.437	0.152 0.266	0.429 0.463	0.339 0.425	0.213 0.326	0.329 0.409	0.344 0.420
	96	<b>0.190</b> <u>0.316</u>	0.377 0.439	1.045 0.886	0.623 0.586	0.453 0.505	<u>0.197</u> <b>0.308</b>	0.853 0.703	0.367 0.441	0.361 0.441	0.572 0.563	0.638 0.602
Avg		<b>0.129</b> <b>0.244</b>	0.230 0.324	0.913 0.801	0.365 0.405	0.295 0.389	<u>0.138</u> <u>0.250</u>	0.472 0.495	0.327 0.418	0.203 0.305	0.297 0.372	0.327 0.397
PEMS07	12	<b>0.059</b> <b>0.157</b>	0.070 0.173	0.068 0.169	0.093 0.206	0.116 0.241	0.075 0.179	0.207 0.335	<u>0.061</u> <u>0.165</u>	0.107 0.178	0.085 0.199	0.096 0.223
	24	<u>0.078</u> <b>0.179</b>	0.109 0.215	0.087 0.190	0.195 0.295	0.209 0.327	0.083 0.198	0.314 0.412	<b>0.071</b> <u>0.177</u>	0.112 0.216	0.149 0.268	0.231 0.360
	48	<u>0.104</u> <b>0.211</b>	0.199 0.296	0.122 0.231	0.485 0.469	0.397 0.456	0.128 0.235	0.595 0.553	<b>0.100</b> <b>0.208</b>	0.168 0.282	0.292 0.383	0.143 0.272
	96	0.128 <b>0.226</b>	0.283 0.341	0.159 0.267	0.979 0.716	0.592 0.552	0.150 0.253	0.556 0.563	<b>0.120</b> <u>0.221</u>	0.275 0.373	0.531 0.535	0.312 0.417
Avg		0.092 <b>0.193</b>	0.165 0.256	0.109 0.214	0.438 0.422	0.329 0.394	0.109 0.216	0.418 0.466	<b>0.088</b> <u>0.192</u>	0.166 0.262	0.264 0.346	0.196 0.318
PEMS08	12	<b>0.076</b> <b>0.178</b>	0.100 0.208	0.081 0.183	0.109 0.222	0.153 0.259	0.158 0.192	0.295 0.391	0.146 0.198	0.096 0.206	0.105 0.219	0.141 0.262
	24	0.124 0.223	0.171 0.279	<u>0.118</u> <u>0.222</u>	0.205 0.306	0.238 0.357	<b>0.112</b> <b>0.219</b>	0.345 0.419	0.171 0.221	0.144 0.256	0.179 0.291	0.243 0.350
	48	<b>0.172</b> <b>0.216</b>	0.317 0.380	<u>0.202</u> 0.292	0.493 0.484	0.473 0.515	0.231 <b>0.198</b>	0.503 0.495	0.220 0.270	0.253 0.351	0.343 0.405	0.439 0.476
	96	<b>0.278</b> <b>0.296</b>	0.468 0.459	0.395 0.415	0.582 0.548	0.748 0.646	<u>0.291</u> 0.338	1.268 0.857	0.285 <u>0.303</u>	0.482 0.492	0.720 0.592	0.886 0.684
Avg		<b>0.162</b> <b>0.228</b>	0.264 0.332	0.199 0.278	0.347 0.390	0.403 0.444	0.198 0.236	0.603 0.541	0.206 0.248	0.244 0.326	0.337 0.377	0.427 0.443

Table 9: Full results of short-term forecasting. All the results are selected from 4 different prediction lengths {12, 24, 48, 96}, and the look-back length is fixed to 96 for all baselines. A lower MSE or MAE indicates a better prediction, with the best in **boldface** and second in underline.

Design	DMSC(Ours)	w/o EMPD	w/o TIB	w/o ASR-MoE	①static decomp	②only $\mathbf{F}_{intra}$	③w/o $\mathbf{F}_{fused}^l$	④Agg. Heads	⑤w/o $\mathcal{E}^g$	⑥w/o $\mathcal{E}^l$		
Metric	MSE	MAE	MSE	MAE	MSE	MAE	MSE	MAE	MSE	MAE	MSE	MAE
Electricity	96	<b>0.138</b> <b>0.223</b>	0.155 0.247	0.155 0.247	0.175 0.267	0.151 0.245	0.161 0.251	0.157 0.250	0.166 0.256	0.160 0.251	0.171 0.259	
	192	<b>0.160</b> <b>0.258</b>	0.170 0.259	0.169 0.259	0.182 0.275	0.163 0.254	0.171 0.261	0.166 0.257	0.177 0.266	0.167 0.259	0.176 0.264	
	336	<b>0.167</b> <b>0.253</b>	0.179 0.270	0.186 0.276	0.192 0.282	0.176 0.271	0.188 0.278	0.186 0.278	0.194 0.283	0.192 0.284	0.202 0.290	
	720	<b>0.213</b> <b>0.299</b>	0.220 0.305	0.228 0.311	0.234 0.317	0.225 0.312	0.228 0.312	0.238 0.321	0.238 0.319	0.245 0.325	0.246 0.328	
Avg		<b>0.170</b> <b>0.258</b>	0.181 0.270	0.185 0.273	0.196 0.285	0.179 0.271	0.187 0.276	0.187 0.277	0.194 0.281	0.191 0.280	0.199 0.285	
Weather	96	<b>0.160</b> <b>0.210</b>	0.161 0.208	0.173 0.216	0.167 0.215	0.160 0.205	0.166 0.210	0.167 0.216	0.173 0.219	0.170 0.219	0.164 0.213	
	192	<b>0.207</b> <b>0.250</b>	0.213 0.253	0.218 0.255	0.216 0.260	0.215 0.253	0.214 0.254	0.213 0.254	0.222 0.260	0.213 0.254	0.213 0.252	
	336	<b>0.253</b> <b>0.284</b>	0.269 0.292	0.274 0.296	0.271 0.297	0.264 0.289	0.269 0.294	0.266 0.291	0.271 0.296	0.273 0.296	0.256 0.287	
	720	<b>0.313</b> <b>0.332</b>	0.349 0.346	0.353 0.343	0.348 0.349	0.342 0.340	0.346 0.343	0.343 0.332	0.352 0.348	0.346 0.344	0.338 0.331	
Avg		<b>0.233</b> <b>0.269</b>	0.248 0.275	0.255 0.278	0.251 0.280	0.245 0.272	0.249 0.275	0.247 0.273	0.255 0.281	0.251 0.278	0.243 0.271	
Traffic	96	<b>0.389</b> <b>0.259</b>	0.479 0.311	0.486 0.318	0.484 0.314	0.443 0.299	0.461 0.303	0.459 0.308	0.494 0.301	0.494 0.320	0.451 0.317	
	192	<b>0.405</b> <b>0.258</b>	0.493 0.316	0.483 0.314	0.491 0.313	0.458 0.300	0.484 0.311	0.473 0.309	0.495 0.308	0.487 0.317	0.486 0.329	
	336	<b>0.398</b> <b>0.286</b>	0.503 0.322	0.490 0.315	0.503 0.318	0.471 0.302	0.493 0.318	0.485 0.311	0.507 0.316	0.505 0.326	0.479 0.317	
	720	<b>0.437</b> <b>0.290</b>	0.538 0.341	0.530 0.337	0.535 0.334	0.542 0.349	0.516 0.327	0.544 0.328	0.531 0.321	0.531 0.334	0.535 0.342	
Avg		<b>0.407</b> <b>0.274</b>	0.503 0.323	0.497 0.321	0.503 0.320	0.479 0.313	0.489 0.315	0.483 0.314	0.510 0.312	0.504 0.324	0.488 0.326	
Solar	96	<b>0.187</b> <b>0.231</b>	0.221 0.260	0.232 0.278	0.242 0.290	0.208 0.255	0.237 0.280	0.240 0.278	0.241 0.284	0.226 0.272	0.234 0.279	
	192	<b>0.216</b> <b>0.261</b>	0.241 0.273	0.264 0.295	0.295 0.324	0.248 0.281	0.281 0.298	0.302 0.316	0.283 0.303	0.279 0.304	0.273 0.303	
	336	<b>0.223</b> <b>0.269</b>	0.264 0.290	0.283 0.306	0.266 0.302	0.261 0.289	0.289 0.309	0.301 0.312	0.289 0.301	0.276 0.296	0.305 0.322	
	720	<b>0.226</b> <b>0.271</b>	0.267 0.288	0.276 0.293	0.282 0.304	0.254 0.280	0.292 0.303	0.264 0.289	0.298 0.306	0.280 0.299	0.289 0.306	
Avg		<b>0.213</b> <b>0.258</b>	0.248 0.278	0.264 0.293	0.271 0.305	0.243 0.276	0.275 0.298	0.277 0.299	0.278 0.299	0.265 0.293	0.275 0.303	

Table 10: Full results of ablation study. All the results are selected from 4 different prediction lengths {96, 192, 336, 720}, and the look-back length is fixed to 96 for all baselines. A lower MSE or MAE indicates a better prediction, with the best in **boldface** and second in underline.